

Controlled Surface Adhesion of Macrophages via Patterned Antifouling Polymer Brushes

Johannes Striebel, Mariia Vorobii, Ravi Kumar, Hui-Yu Liu, Bingquan Yang, Carsten Weishaupt, Cesar Rodriguez-Emmenegger,* Harald Fuchs, Michael Hirtz,* and Kristina Riehemann*

Macrophages will play an important role in future diagnostics and immunotherapies of cancer. However, this demands to selectively capture and sort different subpopulations, which remains a challenge due to their innate ability to bind to a wide range of interfaces indiscriminately. The main obstacle here is the lack of interfaces combining sufficient antifouling properties with the display of specific binding sites allowing sorting and quantification. Herein, as a proof of principle means, it is introduced to pattern interfaces to locally and selective capture macrophages. The repellent coating is based on antifouling polymer brushes, which can be functionalized. Arrays of binding sites are constructed by microchannel cantilever spotting. Those structures are tested for the isolation of different macrophage subtypes, especially polarized anti-inflammatory macrophages of the M2 type which can be found associated to tumors (“tumor associated macrophages”; TAMs). Using macrophages as a model system, it is demonstrated that the newly developed surfaces and patterns are efficient for specifically trapping targeted cells and can be useful for further development of therapeutic or diagnostic purposes in the future.

macrophages can follow two different pathways. This leads to their polarization into two subpopulations with antagonistic properties: 1) classically activated macrophages (M1) that inhibit cell proliferation and cause tissue damage and 2) alternatively activated macrophages (M2) that promote cell proliferation and tissue regeneration.^[2] The balance in this polarization is key in an effective immune response, but dysregulation can cause or aggravate disease.^[3] In particular, some cancers, such as malignant melanoma, can induce polarization turning the macrophages against the healthy tissues. The development of malignant melanoma has been attributed to the presence of specific macrophage subpopulations, which can be found adjacent to tumor tissue.^[4,5] Such “tumor associated macrophages” (TAMs) belong to the subtype M2 which exhibit anti-inflammatory activities.^[6] TAMs can boost tumorigenesis

by supporting proliferation, invasion and metastasis, stimulate angiogenesis, and inhibit antitumor immune response.^[7–9] Accordingly, TAMs are an emerging target for diagnostic purposes^[8,10] and prognosis of disease clinical course.^[11,12] Thus, the development of platforms for selective capture that enable studying the behavior of specific subpopulations of

1. Introduction


Macrophages are an important part of the innate immune system that provides defence to our body from different matter (pathogens, cellular debris, cancer cells, and so on) and support tissue repair.^[1] Depending on their microenvironment,

J. Striebel, Prof. H. Fuchs, Dr. K. Riehemann
Physical Institute and Center for Nanotechnology (CeNTech)
University of Münster
Wilhelm-Klemm-Straße 10, 48149 Münster, Germany
E-mail: riehema@uni-muenster.de

M. Vorobii, Dr. C. Rodriguez-Emmenegger
DWI – Leibniz Institute for Interactive Materials and Institute of
Technical and Macromolecular Chemistry
RWTH Aachen University
Forckenbeckstraße 50, 52074 Aachen, Germany
E-mail: rodriguez@dwil.rwth-aachen.de

Dr. R. Kumar, Dr. H.-Y. Liu, B. Yang, Dr. M. Hirtz
Institute of Nanotechnology (INT) and Karlsruhe Nano
Micro Facility (KNMF)
Karlsruhe Institute of Technology (KIT)
Hermann-von-Helmholtz-Platz 1, 76344 Eggenstein Leopoldshafen,
Germany
E-mail: michael.hirtz@kit.edu

Dr. C. Weishaupt
Department of Dermatology
University Hospital of Münster
Von-Esmarch-Straße 58, 48149 Münster, Germany

 The ORCID identification number(s) for the author(s) of this article can be found under <https://doi.org/10.1002/anbr.202000029>.

© 2020 The Authors. Published by Wiley-VCH GmbH. This is an open access article under the terms of the Creative Commons Attribution License, which permits use, distribution and reproduction in any medium, provided the original work is properly cited.

DOI: 10.1002/anbr.202000029

macrophages are of high interest for diagnostics, treatment, and follow-up of therapies.^[13]

One way to accomplish this task is to introduce surfaces that can selectively capture the targeted cells at precise locations while preventing nonspecific binding of other cells or other subpopulations. The specific capture is usually achieved by introducing receptors or ligands that are complementary to those expressed in the desired cells but orthogonal to others, while the prevention of unspecific adhesion demands to generate physical barriers that repel cells. Nevertheless, surfaces capable of specifically capturing macrophage subpopulations are still lacking.^[14] This can be attributed to 1) the inherent ability of macrophages to unspecifically adhere to a large variety of surfaces, posing a much greater challenge to capture them with specificity and spatial control than other types of cells and 2) surfaces that can repel or attract macrophages [e.g., patterned polyethylene glycol (PEG) hydrogels,^[15–17] or polysaccharides^[18]] offer no discrimination of macrophage subtype and often still suffer a satisfying lack of adhesion contrast between areas that repel and areas that attract macrophages.^[19–24] Thus, also the solution will be twofold, addressing 1) by efficiently suppressing unspecific adhesion and 2) offering highly specific binding capable of addressing macrophage subpopulations selectively.

The key to prevent unspecific adhesion (thus addressing challenge (1)) is on one hand to create a general barrier to cell adhesion and on the other hand to prevent the adsorption of proteins that promote binding of macrophages to the newly developed interface. Two types of mechanisms are in place: adsorption of protein to minimize the interfacial energy between the surface and water (a very unspecific mechanism) and the specific binding of proteins from the complement system that signal macrophages to adhere. In this work, both mechanisms are termed fouling. Not only do these adsorbed proteins act as a conditioning film but also obscure the specific interactions of cells with immobilized receptors.^[25–27] To eliminate the fouling from proteins, different strategies have been developed to minimize or prevent protein adsorption.^[28–30] They are based on reducing the driving force to fouling, for example, using hydrophilic self-assembled monolayers (SAMs) or polymers,^[31,32] using peptides^[33,34] or even protein–polymer hybrids.^[35] Another strategy is the use of superhydrophobic coatings that have extremely low polarizability thus minimizing the driving force for adsorption.^[36,37] Even commonly used coatings based on end-grafted PEG that displayed excellent antifouling properties for single protein solutions such as albumin, failed to prevent fouling from complex biological media such as undiluted blood plasma.^[32] Furthermore, despite the fact that these coatings cannot be easily functionalized, they also induce activation of macrophages and their adsorption.^[38,39] To date, only surface modifications based on polymer brushes, prepared using a grafting-from approach, are able to prevent fouling from both, single protein solutions and complex real biological media, such as saliva, undiluted blood plasma, and blood.^[27,40–43] The high grafting density of the brushes obtained by the grafting-from approach results in coatings that are impenetrable for macromolecules (autophobic effect)^[44] and acts as entropic barrier for adsorption of protein and cells. Hydrophilic polymer brushes reduce the interfacial energy with water and as a result reduce the thermodynamic drive to adhesion. Antifouling polymer brush coatings have been

already implemented in the development of biosensors able to detect biomarkers in undiluted biological media in relevant concentration for clinical diagnostic and food safety.^[45–49] To address challenge (2) and introduce selectivity for subpopulations of macrophages, targeted and site-specific functionalization of the antifouling surface needs to be achieved. Hierarchically structured polymer brushes can combine both—antifouling properties and capability to be functionalized with biomacromolecules.^[45,50] Previously, we reported “clickable” polymer brushes that after biofunctionalization were able to detect analytes in blood plasma without disruption of their antifouling properties.^[51] These brushes consist of two blocks: an antifouling bottom block and an azide-functional top block. The azide groups are able to “click” dibenzocyclooctine or bicyclononyne without any catalyst and immobilize bioreceptors attached to it via catalyst-free strain-promoted alkyne–azide cycloaddition (SPAAC).^[52–54] Simultaneously, the antifouling block prevents any nonspecific protein adsorption. As a result, this surface modification is a model label-free biosensing platform.

In the present work, we aim at demonstrating the basic principle of selective capturing of macrophage subpopulations on array structures. Such studies would pave the road for future applications in diagnostic devices, giving access to ordered arrays of different macrophage subtypes. Maskless lithography can provide the desired feature density and size that will be optimal for selective capture of macrophages while minimizing the overall size of arrays. Recently, we have shown the use of “clickable” antifouling polymer brushes as substrate for polymer pen lithography (PPL)^[55] to generate click chemistry based arrays to capture proteins.^[56] However, microchannel cantilever spotting (μ CS), where femtoliter-scale microdroplets of ink are transferred to a substrate by a cantilever carrying a microfluidic channel,^[57] offer an ideal feature size for our purposes, closely resembling the targeted cell size^[58] and offers high accuracy in the generation of microarrays.^[59] Therefore, μ CS was chosen as lithographic tool in our approach for providing the desired localized highly specific binding places for adhesion of macrophages of different polarization, while preventing unspecific binding of the macrophages and other macromolecules to the substrate.

2. Results and Discussion

For the goal of achieving selective macrophage capture, two key factors have to be considered: 1) specific receptors and 2) nonfouling material. To combine both of these in one approach, hierarchical polymer brushes were utilized.

2.1. Preparation of Polymer Brushes

Hierarchical polymer brushes were synthesized from silicon and glass substrates. The brushes consist of a bottom block (poly(oligoethylene glycol methylether methacrylate)) with repellent properties and a top block which can be functionalized by click chemistry (refer to **Figure 1**). The synthesis of the polymer brushes can be divided into three steps: 1) formation of SAM of initiator, 2) grafting of the antifouling block, and 3) grafting of the azide-functional block. The initiator, 11–(trichlorosilyl)

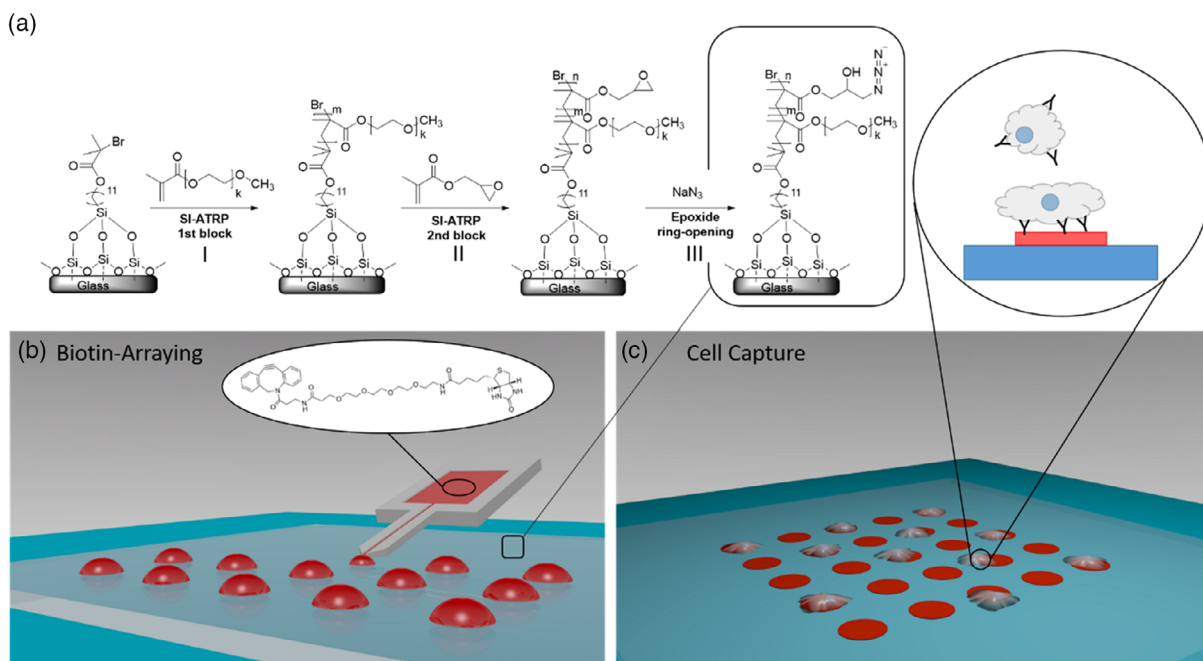


Figure 1. Preparation of microarrays on hierarchical polymer brushes for the selective capture of macrophages. a) Synthesis of polymer brush. b) Microarray generation by μ CS of biotin–DBCO. c) After incubation with streptavidin, cells specifically labeled with biotinylated antibodies are selectively captured on the biotin–streptavidin arrays.

undecyl 2-bromo-2-methylpropanoate, was selected because of its ability to form well-organized and stable monolayers on different substrates.^[60] The polymer brushes were grafted from the initiator layer using surface-initiated atom transfer radical polymerization (SI-ATRP). This type of polymerization provides living end groups which are crucial for successful grafting of the top block. The grafting of each block was monitored by ellipsometry using Si wafer as a model substrate. The dry ellipsometric thickness of the first block was 20 nm, further increasing to 24 nm after grafting of the second block, and remained the same after functionalization of brushes with azide groups (Table S1, Supporting Information).

2.2. Quantification of Macrophage Repellency

The repellence to unspecific macrophage adhesion was first tested via a dot plot of nonpolarized ($M\Phi$), M1, and M2 macrophages. To assess the selectivity, an assay was developed in which some areas of the surfaces are capable of capturing antibody-labeled macrophages while the other remain repellent. The macrophages were incubated with subtype-specific biotinylated antibodies and nonspecific biotinylated IgG for isotype control, prior to the test. This yields the macrophages' surfaces decorated with biotin. To test repellence versus binding, macroscopic spots bearing streptavidin were created, capable of capturing biotin-decorated macrophages, whereas the remaining surface should be nonadhesive. To generate the streptavidin spot, a drop of a biotin-dibenzocyclooctyne (biotin-DBCO) solution was deposited using a pipette on the surface of polymer brushes with azide groups. SPAAC provided fast and efficient immobilization of biotin. Subsequently, the substrates were incubated

with a streptavidin solution, resulting in millimeter-scale streptavidin bearing dots on the surfaces while the rest of them remain with unfunctionalized polymer brushes. Such design allows capturing biotin-bearing cells on the streptavidin-exhibiting area over a biotin–streptavidin–biotin sandwich structure. To test this, the prepared surfaces were incubated with macrophages of different polarizations obtained from cell culture (all macrophages were either incubated with antibodies specific to their respective subtype or (for the control experiments) with an unspecific IgG control antibody). Almost no macrophages adhered on the nonfunctionalized brushes (Figure 2a). On the other hand, streptavidin-bearing polymer brushes after incubation with the macrophages labeled with biotinylated specific antibody showed highly specific binding to the surface (Figure 2b). These demonstrate that polymer brushes are able to prevent unspecific adhesion of highly adherent macrophages while functionalization of brushes with streptavidin leads to increased binding efficiency. Finally, on incubation of the dot-plotted surface with the respective macrophages pre-incubated with control antibody, only minor unspecific binding for $M\Phi$ and M1 and strongly reduced binding of M2 macrophages is observed (Figure 2c). The remaining adhesion of M2 macrophages incubated with IgG can be explained by a slight binding of the IgG control to the macrophages. All cell subtypes exhibit statistically significant binding to the specific antibodies compared with the control areas ($M\Phi$: $P < 0.001$, M1: $P < 0.01$, M2: $P < 0.05$, raw data given in Table S2, Supporting Information). The difference in confidence level could be caused by differences in affinity of the control antibody to the specific antigens at the cell membrane of the specific macrophage. Table 1 shows the efficacy of the brushes in reducing the unspecific adhesion of macrophages. Remarkably, only few macrophages ((5 ± 3) to (6 ± 4) cells on 0.762 mm^2

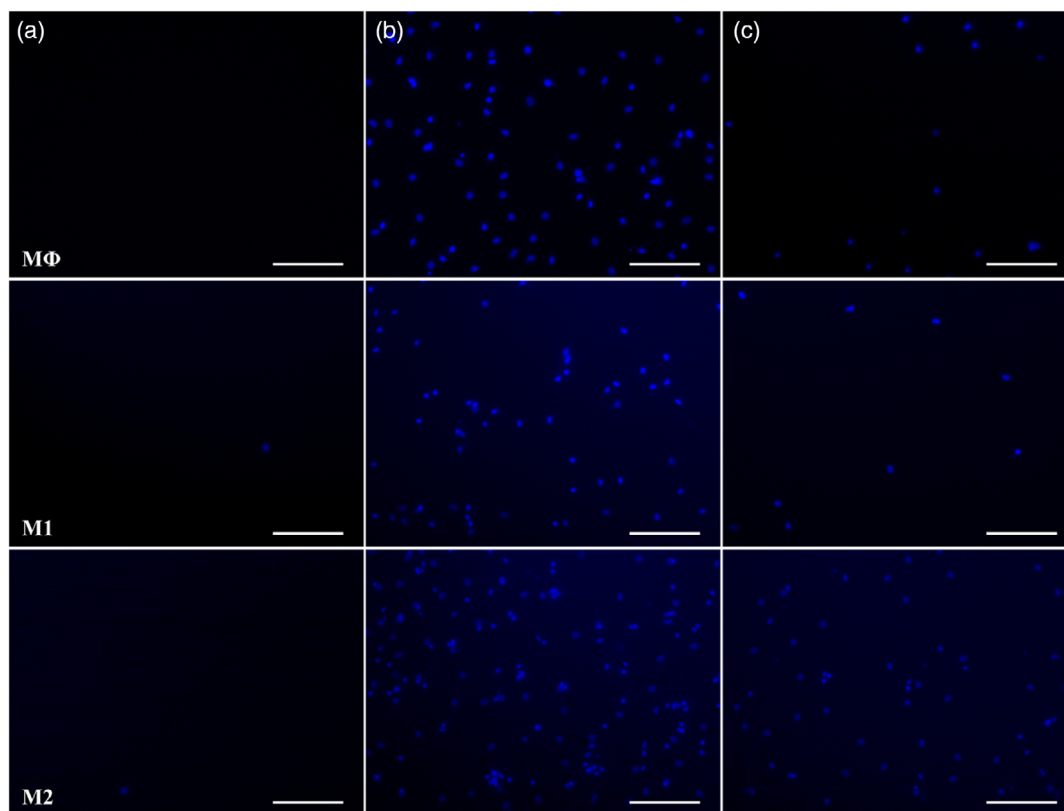


Figure 2. Fluorescence image of a dot plot surface after incubation with biotinylated MΦ, M1, and M2 macrophages. a) Bare antifouling polymer brushes after incubation with macrophages (unspecific binding), b) binding of macrophages incubated with a biotinylated specific antibody to biotin–streptavidin functionalized brushes (specific binding), c) binding of macrophages incubated with biotinylated control IgG to biotin–streptavidin functionalized brushes (control). Cells were stained with DAPI. Scale bars equal 100 μm in each image.

screened, thus only (7 ± 5) cells·mm⁻² in average) adhered unspecifically, compared with specifically captured cells [(174 ± 58) to (421 ± 95) cells on 0.762 mm² screened, thus (228 ± 76) cells·mm⁻² to (552 ± 100) cells·mm⁻²]. These results are especially striking when compared with other standard surfaces and blocking methods, which are not sufficient for efficient macrophage repellence. As controls, commonly used surfaces and different blocking agents were tested: 1) fetal bovine serum (FBS), as a common blocking strategy in biology, 2) SEA BLOCK blocking as used in immunohistochemistry based on adsorption of macromolecules from steelhead salmon fish serum, 3) SEA BLOCK + 1% TWEEN, as well as 4) tissue culture plates (as positive

Table 1. Comparison in cell count of specific and unspecific binding potential of surfaces functionalized by polymer brushes. Numbers represent number of cells per 0.762 mm² area. For each value, at least four different areas on a dot plot were averaged and the standard deviation was calculated. Results are statistically significant (*t*-test, *P* < 0.05).

	Unspecific binding	Specific antibody	IgG control
MΦ	6 ± 4	228 ± 78	66 ± 42
M1	5 ± 3	174 ± 58	56 ± 14
M2	6 ± 4	421 ± 95	247 ± 75

control/comparison). As shown in Figure S1, Supporting Information, all these blocking strategies failed to prevent adsorption of macrophages.

2.3. Specific Macrophage Adhesion

The localized specific capture of macrophages was explored by generating microarrays with binding sites supporting a biotin–streptavidin sandwich structure. A microspotting approach was used to locally functionalize the polymer brush with biotin–DBCO. This allows subsequent streptavidin binding that acts as capture site for biotinylated-antibody bearing macrophages. Typically, arrays of 20 × 20 dot features were spotted via μCS, which deposits small femtoliter-sized droplets on a surface.^[57] These droplets can act as reaction vessels where click-reactions take place.^[58,61,62] After 20 min of binding, the excess ink was washed away and samples were incubated with fluorescently labeled streptavidin to activate the array for macrophage capture. A typical result of the arraying procedure is shown in Figure 3. The arrays used in our studies consist of spots with a radius of (7.0 ± 0.6) μm (derived from the measured area per spot of $[154.5 \pm 25.1]$ μm² and assuming a circular shape) and a center-to-center distance (pitch) of 50 μm spanning over a square millimeter.

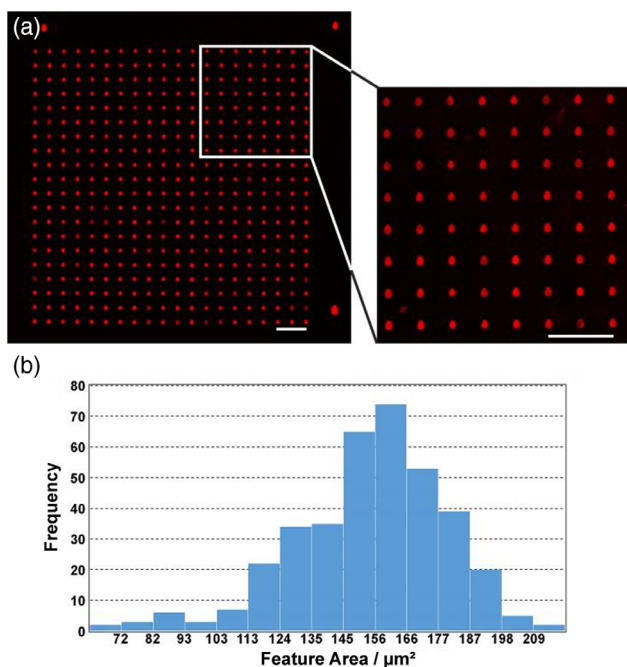


Figure 3. a) Streptavidin microarrays for cell capture. Biotin was printed by μ CS on the polymer brushes. Streptavidin-Cy3 was then incubated on the substrate. Scale bar is 100 μ m in both images. b) Histogram of feature size in the macrophage capture array. Average feature area (calculated from 370 features in eight different images) is $(154.5 \pm 25.1) \mu\text{m}^2$. Assuming a circular shape of the features, this area corresponds to a radius of $(7.0 \pm 0.6) \mu\text{m}$.

In our studies, we focused on the feasibility of specific capture of polarized macrophages as they are the most important target for medical application. M1 macrophages comprise inflammatory and antitumoral effects, whereas the anti-inflammatory M2 macrophages support tumor growth.^[63] The macrophages were either incubated with respective specific biotinylated antibody or with an (also biotinylated) nonspecific IgG control antibody and then incubated on the capture arrays. After washing and staining, the capture arrays and adhering cells were imaged by fluorescence microscopy (Figure 4). A high correlation of captured macrophages with the array features is observed on visual inspection (Figure 4a,b). Fewer cells were observed on the capture array of macrophages incubated with the nonspecific IgG control, compared with incubation with specific antibodies. To quantify the cell capture, cells on a capture spot were counted in comparison to cells attached to the unmodified surface. This results in a cell count of 217 cells on feature versus 56 unspecifically bound for M1 macrophages, and 203 cells on feature versus 32 unspecifically bound cells for M2 macrophages. For the IgG control samples (Figure 4c), a total cell count of 82 (55 cells on feature vs 27 in between features) for M1 macrophages, and 23 cells (12 on feature vs 11 in between features) for M2 macrophages was observed. These results show the high specificity of macrophage capture, as shown in the ratio of on feature (specific capture) to total cell count being 79.5% for M1 and 86.4% for M2 macrophages pre-incubated with specific antibodies. Furthermore, the total cell count is 3.3 times higher for M1 and 10.2 times for M2 macrophages, respectively, using specific antibody versus the IgG controls (raw cell counts given in Table S3, Supporting

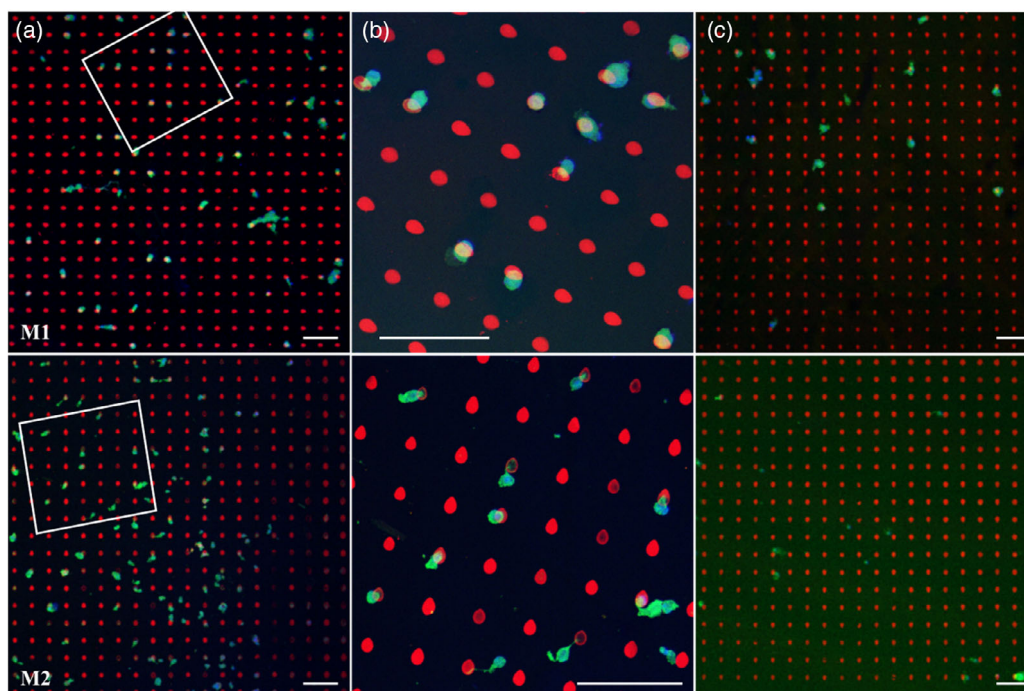


Figure 4. Selective capture of polarized M1 and M2 macrophages on microarrays. The cells were incubated with biotinylated antibodies in form of specific and nonspecific IgG (as isotype control) prior to the test. a) Localized capture of macrophages incubated with biotinylated specific antibodies on microarrays. b) Zoom-in of the areas (white frames) in (a) of the corresponding macrophage subtype. c) Binding of macrophages on microarrays incubated with nonspecific biotinylated IgG (isotype control). Cells were stained with DAPI and CTOG, arrays with Cy-3. Scale bars are 100 μ m in all pictures.

Information). Moreover, the capture approach works also when cells are not incubated with biotinylated antibody beforehand but the antibody is put on the substrate's capture features instead (Figure S3, Supporting Information)—which can be exploited for multiplexed (i.e., more than one macrophage subtype) selective cell adhesion within one array. The intrinsic distinction between specifically bound (co-located with array feature) and unspecifically bound (in between features) can additionally be used in cell-picking applications to ensure low false-positive counts, as unspecifically bound macrophages can be easily excluded.

3. Conclusion

Our studies demonstrated that the hierarchical antifouling polymer brushes could repel the adhesion of macrophages, one of the most adherent cell types.^[25,26] Furthermore, the polymer brushes were functionalized to introduce specific capture arrays based on biotin–DBCO immobilization with subsequent macrophage capture over a biotin–streptavidin–biotin sandwich. The resulting arrays show good specificity for macrophage capture based on specific antibody interaction and offer additional control for false positives (in the form of unspecifically adhering cells) by checking co-location of array features with adhering macrophages. Such arrays could be upscaled for high-throughput production by additional printing methods as μ CS with parallel tips^[64] or PPL^[56,65] with adjusted custom stamps of appropriate feature size, and be incorporated into microfluidics for future application in biomedical experiments and clinical diagnostics.^[65–67] Overall, the approach opens up the route for easy and efficient macrophage capture and future sorting applications in research and medical practice.

4. Experimental Section

Materials: Oligo(ethylene glycol) methyl ether methacrylate (MeOEGMA, $M_n = 300 \text{ g mol}^{-1}$), glycidyl methacrylate ($\geq 97.0\%$, GMA), CuBr_2 (99.999% trace metals basis), CuBr (99.999% trace metals basis), 2,2'-bipyridyl ($\geq 99\%$ BiPy), sodium azide ($\geq 99\%$, ultra dry, NaN_3) were purchased from Sigma-Aldrich, Germany. Toluene (99.85%), *N,N*-dimethylformamide (99.8%, DMF) and dichloromethane (99.9%, CH_2Cl_2) extra dry over molecular sieve were purchased from Acros Organic, Germany. Methanol (MeOH), ethanol (EtOH), acetone, and toluene were purchased from VWR Chemicals, Germany. Aluminum oxide 90 basic was purchased from Carl Roth, Germany. Milli-Q water was obtained using Elga USA filter Purelab Plus UF purification system (PL5113 02), UK 11-(trichlorosilyl)undecyl 2-bromo-2-methylpropanoate, was synthesized according to the modified method from literature.^[68,69]

Substrate Activation and Immobilization of Initiator: Round glass substrates (15 mm diameter) were rinsed twice with EtOH and Milli-Q water, dried with N_2 , and activated inside a vacuum plasma cleaning machine (TePla PS100, Germany). The duration of treatment was 20 min with oxygen flow of 40 mL min^{-1} and micro wave power of 200 W. Immediately after, the substrates were immersed in a freshly prepared solution of 11-(trichlorosilyl)undecyl 2-bromo-2-methylpropanoate in dry toluene (1 mg mL^{-1}). The silanization was allowed to proceed for 3 h in a dry environment to form SAM of initiator. The substrate were rinsed with toluene, acetone, EtOH, and Milli-Q water and dried with N_2 .

Grafting of Polymer Brushes: The hierarchically structured polymer brushes consisting of two blocks were synthesized using a protocol reported previously.^[51] A brief description of the procedure is: 1) For

the preparation of an antifouling block, 15 mL of MeOH and a monomer solution [MeOEGMA (14.2 g, 47.4 mmol) in 12.5 mL of Milli-Q water] were placed in two separate round-bottom flasks and degassed by bubbling N_2 for 1 h. After degassing, 12.5 mL of MeOH was transferred to previously degassed flask containing catalyst (BiPy (386.8 mg, 2.5 mmol), CuBr_2 (41.9 mg, 188 μmol), and CuBr (134.6 mg, 938 μmol)) under N_2 atmosphere and stirred until complete dissolution. Subsequently, the monomer and the catalyst solutions were mixed by transferring the solution using a gas-tight syringe under N_2 protection. The obtained polymerization mixture was transferred under N_2 atmosphere to previously degassed reactor containing substrates with SAM of initiator. The polymerization was carried out at 30°C for 20 min and stopped by adding Milli-Q water. The substrates were rinsed twice with EtOH and Milli-Q water and dried with N_2 . 2) For the preparation of an azide-functional block, GMA was passed through the basic alumina column to remove inhibitor. Then, obtained GMA (16.7 g, 117.6 mmol), BiPy (458 mg, 2.9 mmol) CuBr_2 (52.5 mg, 235 μmol), and dry DMF (24 mL) were placed in a round-bottom flask and degassed for 1 h by bubbling N_2 . Subsequently, CuBr (168.4 mg, 1.2 mmol) was added to the flask under N_2 protection and stirred until complete dissolution. The obtained polymerization mixture was transferred to previously degassed reactor containing substrates with MeOEGMA block, used as macroinitiator. The polymerization was allowed to proceed at 30°C for 4 h and was stopped by removing samples from the reactor. The substrates were rinsed twice with dry DMF and dry CH_2Cl_2 and dried with N_2 . Afterward, the slides with obtained diblock polymer brushes were immersed in 40 mL solution of NaN_3 (3.4 mg mL^{-1}) in dry DMF to functionalize the GMA block with azide groups. The reaction was carried out at 60°C for 24 h. The samples were washed with DMF, EtOH, and Milli-Q water and dried with N_2 .

Preparation of Dot Plot Substrates: Ink was prepared by mixing biotin-PEG4-DBCO (2 mg mL^{-1} in DMSO) (Jena Bioscience, Germany) with 87% glycerol (7:3) (Sigma Aldrich, Germany). Substrates were activated for cell capture by pipetting 0.5 μL ink onto substrates. The reaction was carried out on a hotplate for 20 min at 37°C . Substrates were then washed three times with phosphate buffer saline (PBS). Obtained samples were incubated with 100 μL of 1 mg mL^{-1} streptavidin-Cy3 (Sigma-Aldrich, Germany) in PBS (1:100) right before cell capture experiments for 1 h at room temperature and washed two times with PBS.

Printing of Capture Arrays: Spotting of the binding sites was implemented with surface patterning tool (SPT) probes^[70] (SPT-S-C10S, Bioforce Nanosciences, USA) on a NLP 2000 system (NanoInk, USA) with a self-made custom tip holder. The SPTs were rendered hydrophilic by oxygen plasma treatment at 0.2 mbar, 100% O_2 , 200 W, for 2 min in an Atto plasma cleaner (Diener Electronic, Germany) immediately before use. Ink for μCS was prepared as described in the previous section. Arrays had dimensions of 20×20 dots with a pitch of 50 μm in each direction. Typical conditions for spotting were a dwell time of 0.1 s and a relative humidity of 20%. After printing substrates were incubated for 20 min at 37°C , washed and incubated with streptavidin-Cy3 as described in the previous section.

Macrophage Isolation and Cultivation: Human monocytes were isolated from buffy coats from peripheral blood of healthy volunteers obtained from the Red Cross by Ficoll gradient centrifugation. Cells were purified via the monocyte specific surface marker cluster of differentiation 14 (CD14). This was done using Magnetic Activated Cell Sorting (MACS, Miltenyi Biotec GmbH, Bergisch Gladbach, Germany). The purity of CD14 positive cells was at least 95% determined by flow cytometry in an Agilent 2100 Bioanalyzer (Agilent Technologies, Germany).

The obtained cells were cultured in McCoy's 5A medium supplemented with 15% FBS, 1% L-glutamine, and 2% nonessential amino acids (all obtained from Biochrom, Germany). The tests were performed after the polarization to M1 or M2 macrophages or with unpolarized macrophages (M Φ).

Macrophage Polarization: After isolation and cultivation, cells were differentiated as described earlier.^[2,71] Briefly, for M1 polarization, cells were incubated for 6 days with 50 ng mL^{-1} granulocyte–macrophage colony-stimulating factor (GM-CSF) from *E. coli* (Invitrogen/Thermo Fisher Scientific, Germany) in culture medium. Then cells were cultured for 24 h with 50 ng mL^{-1} lipopolysaccharide (LPS) (clone: *E. coli* O55:B5,

Sigma-Aldrich, Germany) and 20 ng mL⁻¹ interferon gamma (IFN γ) from *E. coli* (Invitrogen/Thermo Fisher Scientific, Germany). For M2 polarization, cells were incubated for 6 days at 37 °C and 5% CO₂ with 50 ng mL⁻¹ macrophage colony-stimulating factor (M-CSF) from mammalian (Invitrogen/Thermo Fisher Scientific, Germany) in culture medium. Subsequently, cells were cultivated for 24 h with 20 ng mL⁻¹ interleukin-4 (IL-4) and 20 ng mL⁻¹ interleukin-13 (IL-13) both from *E. coli* (Invitrogen/ThermoFischer, Germany), also in culture medium. To obtain undifferentiated macrophages, the monocytes were cultured for 6 days with 50 ng mL⁻¹ of M-CSF in the culture medium.

Cell Adhesion Experiments: To investigate the reaction of cells to different surface structures, the macrophages were removed from the cell culture plate and grown on the respective surface for 12 h in PBS without any cytokines added. For microscopic analysis, cells were fixed by incubation with 4% paraformaldehyde solution for 10 min.

Preparation of Biotin-Labeled Macrophages: During the relevant experimental setups, cells were pre-incubated with cell-specific biotinylated antibodies prior to the attachment to the streptavidin-activated repellent surfaces.

Three types of biotinylated antibodies were used: For nonpolarized macrophages, biotinylated anti-CD14 (clone: 61D3, Invitrogen/Thermo Fisher Scientific, Germany) was used. For the M1 subtype, biotinylated anti-CD80 (clone: 2D10.4, Invitrogen/Thermo Fisher Scientific, Germany) was chosen. For capturing cells with a M2 subtype, biotinylated anti-CD163 (clone: eBioGHI/51, Invitrogen/Thermo Fisher Scientific, Germany) was applied. Controls were performed using biotinylated IgG1 kappa isotype control antibody (clone: P3.6.2.8.1, Invitrogen/Thermo Fisher Scientific, Germany). Per substrate of 15 mm diameter, 10⁶ cells were incubated with 1 μ g of antibody in 100 μ L BSA/PBS 0.1% w/v for 1 h at 37 °C on a shaker. Then, cells were centrifuged for 7 min at 1000 rpm and resuspended in 100 μ L warm PBS and given on the functionalized substrate.

Direct Incubation of Cells: Substrates were prepared as described earlier. They were then incubated with biotinylated antibodies corresponding to the target cell type (see earlier section). 1 μ g of antibody in 100 μ L PBS was incubated on the substrates for 1 h at room temperature. Then, cells were washed two times with PBS. 10⁶ cells per substrate were then centrifuged and resuspended in 100 μ L warm PBS. Incubation of cells on the surface started directly after antibodies were attached.

Spectroscopic Ellipsometry: Si wafers were used as a model substrate to determine thickness of the polymer brushes. The dry ellipsometric thickness was measured using an OMT Ellipsometer and was analyzed using VisuEl software version 3.4.1, Optische Messtechnik GmbH. Ellipsometric data were measured in air at room temperature in the wavelength range $\lambda = 460\text{--}870$ nm at the angle of incidence of 70°.

Optical Microscopy: For microscopy, cells were stained with 4',6-diamidino-2-phenylindole (DAPI) (1:1000) and Cell Trace Oregon Green (CTOG) (2.5 μ g mL⁻¹) (Invitrogen/Thermo Fisher Scientific, Germany) after fixation. Samples were analyzed using a fluorescence microscope Nikon Eclipse TE2000-U (Nikon, Japan) and a Leica TCS SP8 confocal laser scanning microscope (Leica, Germany) using a hybrid-detector. All pictures were taken with a 10 \times objective. Depending on the experimental setup, DAPI, Fluorescein (FITC), and Cy3 channels were used.

Evaluation of Array Feature Size: The feature size in the printed arrays was obtained by analyzing eight different images bearing 370 features using the software ImageJ.^[72,73] The images were first thresholded and features detected by the "find particle" function, then feature areas were extracted. Based on the feature area, feature radii were calculated (assuming a circular shape) as

$$r = \sqrt{A/\pi} \quad (1)$$

where A is the area of the features and r is the corresponding radius. The error ranges reported in area and radius correspond to one standard deviation.

Cell Counting for Dot Plots and Capture Arrays: Cell counting in the dot plot experiments was done by counting the number of adherent cells in images corresponding to an area of 0.762 mm² of the unfunctionalized

polymer brush surface (unspecific binding), on the dot plots functionalized with cell-specific antibodies and the dot plots functionalized with the IgG control antibody. For each case, at least four different areas were analyzed, averaged, and the standard deviation calculated. To check for statistical significance, a Student's t -test was performed on the data.

For evaluation of the specific binding on the capture arrays, images from three samples each for M1/M2 capture containing about 1200 array features were counted for cells sitting "on feature" (i.e., the cell counted is co-located with an array feature) versus cells sitting "off feature" (i.e., in between features in the area of the array). The same procedure was repeated for images from two samples each for the M1/M2 IgG control samples.

Supporting Information

Supporting Information is available from the Wiley Online Library or from the author.

Acknowledgements

This work was partly carried out with the support of the Karlsruhe Nano Micro Facility (KNMF, www.knmf.kit.edu), a Helmholtz Research Infrastructure at Karlsruhe Institute of Technology (KIT, www.kit.edu). M.V. and C.R.-E. acknowledge the support of Deutsche Forschungsgemeinschaft (DFG) in the framework of the priority programme 2014 "Towards an Implantable Lung", project number: 346972946 and financial support by German Federal Ministry of Education and Research (BMBF) for the project FeedPlatePlus within the "Neue Produkte für die Bioökonomie" program (grant no. 031B0652). The authors thank Judith Schmidt and Jana Salich, CeNTech, Münster, for dedicated technical assistance, and the authors are grateful for the vast support of the Fluorescence Microscopy Facility Münster under Prof. Jürgen Klingauf and especially for the help of Jana Hüve and Felix Neumann with confocal microscopy.

Conflict of Interest

The authors declare no conflict of interest.

Keywords

antifouling, macrophages, microarrays, microchannel cantilever spotting, polymer brushes

Received: September 3, 2020

Revised: October 14, 2020

Published online:

- [1] D. Hirayama, T. Iida, H. Nakase, *Int. J. Mol. Sci.* **2017**, *19*, 92.
- [2] P. J. Murray, *Annu. Rev. Physiol.* **2017**, *79*, 541.
- [3] L. Cassetta, E. Cassol, G. Poli, *Sci. World J.* **2011**, *11*, 2391.
- [4] M. R. Hussein, E. E. Abu-Dief, A. T. Abou El-Ghait, M. A. Adly, M. H. Abdelraheem, *Int. J. Exp. Pathol.* **2006**, *87*, 237.
- [5] Y. Komohara, Y. Fujiwara, K. Ohnishi, M. Takeya, *Adv. Drug Deliv. Rev.* **2016**, *99*, 180.
- [6] A. Sica, T. Schioppa, A. Mantovani, P. Allavena, *Eur. J. Cancer* **2006**, *42*, 717.
- [7] S. I. Grivennikov, F. R. Greten, M. Karin, *Cell* **2010**, *140*, 883.
- [8] L. Yang, Y. Zhang, *J. Hematol. Oncol.* **2017**, *10*, 58.
- [9] J. Zhou, Z. Tang, S. Gao, C. Li, Y. Feng, X. Zhou, *Front. Oncol.* **2020**, *10*, 188.

- [10] F. Wang, L. Yang, Q. Gao, L. Huang, L. Wang, J. Wang, S. Wang, B. Zhang, Y. Zhang, *Cancer Immunol. Immunother.* **2015**, *64*, 965.
- [11] M. Heusinkveld, S. H. van der Burg, *J. Transl. Med.* **2011**, *9*, 216.
- [12] L. Yang, F. Wang, L. Wang, L. Huang, J. Wang, B. Zhang, Y. Zhang, *Oncotarget* **2015**, *6*, 10592.
- [13] H.-F. Wang, Y. Liu, T. Wang, G. Yang, B. Zeng, C. Zhao, *ACS Biomater. Sci. Eng.* **2020**, *6*, 5040.
- [14] A. Klinder, J. Markhoff, A. Jonitz-Heincke, P. Sterna, A. Salamon, R. Bader, *Exp. Ther. Med.* **2019**, *17*, 2004.
- [15] P. Krsko, K. Vartanian, H. Geller, M. Libera, in *Proc. IEEE 31st Annu. Northeast Bioeng. Conf.*, IEEE, Piscataway, NJ **2005**, pp. 4–6.
- [16] P. Ghosh, M. L. Amirpour, W. M. Lackowski, M. V. Pishko, R. M. Crooks, *Angew. Chem. Int. Ed.* **1999**, *38*, 1592.
- [17] P. Krsko, K. Vartanian, H. Geller, M. Libera, *MRS Proc.* **2004**, *845*, AA8.7.
- [18] I. Y. Tsai, C.-C. Kuo, N. Tomczyk, S. J. Stachelek, R. J. Composto, D. M. Eckmann, *Soft Matter* **2011**, *7*, 3599.
- [19] K. M. DeFife, E. Colton, Y. Nakayama, T. Matsuda, J. M. Anderson, *J. Biomed. Mater. Res.* **1999**, *45*, 148.
- [20] W. J. Kao, J. A. Hubbell, J. M. Anderson, *J. Mater. Sci. Mater. Med.* **1999**, *10*, 601.
- [21] C. R. Jenney, J. M. Anderson, *J. Biomed. Mater. Res.* **1999**, *44*, 206.
- [22] T. O. Collier, J. M. Anderson, W. G. Brodbeck, T. Barber, K. E. Healy, *J. Biomed. Mater. Res. A* **2004**, *69*, 644.
- [23] E. F. Irwin, K. Saha, M. Rosenbluth, L. J. Gamble, D. G. Castner, K. E. Healy, *J. Biomater. Sci. Polym. Ed.* **2008**, *19*, 1363.
- [24] D. Septiadi, A. Lee, M. Spuch-Calvar, T. L. Moore, G. Spiaggia, W. Abdussalam, L. Rodriguez-Lorenzo, P. Taladriz-Blanco, B. Rothen-Rutishauser, A. Petri-Fink, *Adv. Funct. Mater.* **2020**, 2002630.
- [25] M. Shen, T. A. Horbett, *J. Biomed. Mater. Res.* **2001**, *57*, 336.
- [26] M. L. Godek, R. Michel, L. M. Chamberlain, D. G. Castner, D. W. Grainger, *J. Biomed. Mater. Res. A* **2009**, *88*, 503.
- [27] C. Rodriguez-Emmenegger, E. Brynda, T. Riedel, M. Houska, V. Šubr, A. B. Alles, E. Hasan, J. E. Gautrot, W. T. S. Huck, *Macromol. Rapid Commun.* **2011**, *32*, 952.
- [28] I. Banerjee, R. C. Pangule, R. S. Kane, *Adv. Mater.* **2011**, *23*, 690.
- [29] C. Blaszykowski, S. Sheikh, M. Thompson, *Chem. Soc. Rev.* **2012**, *41*, 5599.
- [30] V. B. Damodaran, N. S. Murthy, *Biomater. Res.* **2016**, *20*, 18.
- [31] S. Chen, L. Li, C. Zhao, J. Zheng, *Polymer* **2010**, *51*, 5283.
- [32] T. Riedel, Z. Riedelová-Reichelová, P. Májek, C. Rodriguez-Emmenegger, M. Houska, J. E. Dyr, E. Brynda, *Langmuir* **2013**, *29*, 3388.
- [33] R. Chelmowski, S. D. Köster, A. Kerstan, A. Prekelt, C. Grunwald, T. Winkler, N. Metzler-Nolte, A. Terfort, C. Wöll, *J. Am. Chem. Soc.* **2008**, *130*, 14952.
- [34] S. Chen, Z. Cao, S. Jiang, *Biomaterials* **2009**, *30*, 5892.
- [35] S. Dedisch, F. Obstals, A. de los Santos Pereira, M. Bruns, F. Jakob, U. Schwaneberg, C. Rodriguez-Emmenegger, *Adv. Mater. Interfaces* **2019**, 1900847.
- [36] J. Li, E. Ueda, D. Paulssen, P. A. Levkin, *Adv. Funct. Mater.* **2019**, *29*, 1802317.
- [37] J. Jeevahan, M. Chandrasekaran, G. Britto Joseph, R. B. Durairaj, G. Mageswaran, *J. Coatings Technol. Res.* **2018**, *15*, 231.
- [38] N. Luo, J. K. Weber, S. Wang, B. Luan, H. Yue, X. Xi, J. Du, Z. Yang, W. Wei, R. Zhou, G. Ma, *Nat. Commun.* **2017**, *8*, 14537.
- [39] V. E. Wagner, J. D. Bryers, *J. Biomed. Mater. Res.* **2003**, *66A*, 62.
- [40] A. de los Santos Pereira, C. Rodriguez-Emmenegger, F. Surman, T. Riedel, A. B. Alles, E. Brynda, *RSC Adv.* **2014**, *4*, 2318.
- [41] S. Jiang, Z. Cao, *Adv. Mater.* **2010**, *22*, 920.
- [42] O. Pop-Georgievski, C. Rodriguez-Emmenegger, A. de los Santos Pereira, V. Proks, E. Brynda, F. Rypáček, *J. Mater. Chem. B* **2013**, *1*, 2859.
- [43] B. Xu, C. Feng, Y. Lv, S. Lin, G. Lu, X. Huang, *ACS Appl. Mater. Interfaces* **2020**, *12*, 1588.
- [44] L. Leibler, A. Mourran, *MRS Bull.* **1997**, *22*, 33.
- [45] A. de los Santos Pereira, T. Riedel, E. Brynda, C. Rodriguez-Emmenegger, *Sensors Actuators B Chem.* **2014**, *202*, 1313.
- [46] T. Riedel, F. Surman, S. Hageneder, O. Pop-Georgievski, C. Noehammer, M. Hofner, E. Brynda, C. Rodriguez-Emmenegger, J. Dostálek, *Biosens. Bioelectron.* **2016**, *85*, 272.
- [47] T. Riedel, S. Hageneder, F. Surman, O. Pop-Georgievski, C. Noehammer, M. Hofner, E. Brynda, C. Rodriguez-Emmenegger, J. Dostálek, *Anal. Chem.* **2017**, *89*, 2972.
- [48] H. Vaisocherová-Lísalová, I. Višová, M. L. Ermini, T. Špringer, X. C. Song, J. Mrázek, J. Lamačová, N. Scott Lynn, P. Šedivák, J. Homola, *Biosens. Bioelectron.* **2016**, *80*, 84.
- [49] C. Rodriguez-Emmenegger, O. A. Avramenko, E. Brynda, J. Skvor, A. B. Alles, *Biosens. Bioelectron.* **2011**, *26*, 4545.
- [50] A. de los Santos Pereira, N. Yu Kostina, M. Bruns, C. Rodriguez-Emmenegger, C. Barner-Kowollik, *Langmuir* **2015**, *31*, 5899.
- [51] V. Parrillo, A. Pereira, T. Riedel, C. Rodriguez-Emmenegger, *Anal. Chim. Acta* **2017**, *971*, 78.
- [52] N. J. Agard, J. A. Prescher, C. R. Bertozzi, *J. Am. Chem. Soc.* **2004**, *126*, 15046.
- [53] X. Ning, R. P. Temming, J. Dommerholt, J. Guo, D. B. Ania, M. F. Debets, M. A. Wolfert, G.-J. Boons, F. L. van Delft, *Angew. Chemie Int. Ed.* **2010**, *49*, 3065.
- [54] N. Subramanian, J. B. Sreemanthula, B. Balaji, J. R. Kanwar, J. Biswas, S. Krishnakumar, *Chem. Commun.* **2014**, *50*, 11810.
- [55] F. Huo, Z. Zheng, G. Zheng, L. R. Giam, H. Zhang, C. A. Mirkin, *Science* **2008**, *321*, 1658.
- [56] U. Bog, A. de los Santos Pereira, S. L. Mueller, S. Havenridge, V. Parrillo, M. Bruns, A. E. Holmes, C. Rodriguez-Emmenegger, H. Fuchs, M. Hirtz, *ACS Appl. Mater. Interfaces* **2017**, *9*, 12109.
- [57] G. Arrabito, V. Ferrara, A. Ottaviani, F. Cavaleri, S. Cubisino, P. Cancemi, Y. P. Ho, B. R. Knudsen, M. S. Hede, C. Pellerito, A. Desideri, S. Feo, B. Pignataro, *Langmuir* **2019**, *35*, 17156.
- [58] M. Hirtz, A. M. Greiner, T. Landmann, M. Bastmeyer, H. Fuchs, *Adv. Mater. Interfaces* **2014**, *1*, 1300129.
- [59] J. Atwater, D. S. Mattes, B. Streit, C. von Bojničić-Kninski, F. F. Loeffler, F. Breitling, H. Fuchs, M. Hirtz, *Adv. Mater.* **2018**, *30*, 1801632.
- [60] F. Obstals, M. Vorobii, T. Riedel, A. de los Santos Pereira, M. Bruns, S. Singh, C. Rodriguez-Emmenegger, *Macromol. Biosci.* **2018**, *18*, 1.
- [61] S. M. M. Dadfar, S. Sekula-Neuner, U. Bog, V. Trouillet, M. Hirtz, *Small* **2018**, *14*, 1800131.
- [62] S. M. M. Dadfar, S. Sekula-Neuner, V. Trouillet, M. Hirtz, *Adv. Mater. Interfaces* **2018**, *5*, 1801343.
- [63] S. K. Biswas, A. Mantovani, *Nat. Immunol.* **2010**, *11*, 889.
- [64] J. Xu, M. Lynch, S. Nettikadan, C. Mosher, S. Vegasandra, E. Henderson, *Sensors Actuators B Chem.* **2006**, *113*, 1034.
- [65] H. Liu, C. Koch, A. Haller, S. A. Joosse, R. Kumar, M. J. Vellekoop, L. J. Horst, L. Keller, A. Babayan, A. V. Failla, J. Jensen, S. Peine, F. Keplinger, H. Fuchs, K. Pantel, M. Hirtz, *Adv. Biosyst.* **2020**, *4*, 1900162.
- [66] F. Brinkmann, M. Hirtz, A. Haller, T. M. Gorges, M. J. Vellekoop, S. Riethdorf, V. Müller, K. Pantel, H. Fuchs, *Sci. Rep.* **2015**, *5*, 15342.
- [67] R. Kumar, A. Bonicelli, S. Sekula-Neuner, A. C. B. Cato, M. Hirtz, H. Fuchs, *Small* **2016**, *12*, 5330.
- [68] K. Matyjaszewski, P. J. Miller, N. Shukla, B. Immaraporn, A. Gelman, B. B. Luokala, T. M. Siclovan, G. Kickelbick, T. Valiant, H. Hoffmann, T. Pakula, *Macromolecules* **1999**, *32*, 8716.

- [69] C. Rodriguez-Emmenegger, S. Janel, A. de los Santos Pereira, M. Bruns, F. Lafont, *Polym. Chem.* **2015**, *6*, 5740.
- [70] J. Xu, M. Lynch, J. L. Huff, C. Mosher, S. Vengasandra, G. Ding, E. Henderson, *Biomed. Microdev.* **2004**, *6*, 117.
- [71] S. Gordon, *Nat. Rev. Immunol.* **2003**, *3*, 23.
- [72] C. T. Rueden, J. Schindelin, M. C. Hiner, B. E. DeZonia, A. E. Walter, E. T. Arena, K. W. Eliceiri, *BMC Bioinform.* **2017**, *18*, 529.
- [73] C. A. Schneider, W. S. Rasband, K. W. Eliceiri, *Nat. Methods* **2012**, *9*, 671.